HHS Public Access

Author manuscript

Neuroimage. Author manuscript; available in PMC 2016 June 01.

Published in final edited form as:

Neuroimage. 2015 June ; 113: 153–163. doi:10.1016/j.neuroimage.2015.03.028.

Prestimulus EEG Alpha Oscillations Modulate Task-Related fMRI BOLD Responses to Auditory Stimuli

Jennifer M. Walz[a], **Robin I. Goldman**[b], **Michael Carapezza**[a], **Jordan Muraskin**[a], **Truman R. Brown**[c], and **Paul Sajda**[a,*]

[a]Department of Biomedical Engineering, Columbia University, New York, NY, USA 10027

[b]Waisman Laboratory for Brain Imaging and Behavior, University of Wisconsin–Madison, Madison, WI, USA 53705

[c]Medical University of South Carolina, Charleston, SC, USA 29425

Abstract

EEG alpha-band activity is generally thought to represent an inhibitory state related to decreased attention and play a role in suppression of task-irrelevant stimulus processing, but a competing hypothesis suggests an active role in processing task-relevant information – one in which phase dynamics are involved. Here we used simultaneous EEG-fMRI and a whole-brain analysis to investigate the effects of prestimulus alpha activity on the event-related BOLD response during an auditory oddball task. We separately investigated the effects of the posterior alpha rhythm's power and phase on activity related to task-relevant stimulus processing and also investigated higher-level decision-related processing. We found stronger decision-related BOLD activity in areas late in the processing stream when subjects were in the high alpha power state prior to stimulus onset, but did not detect any effect in primary sensory regions. Our phase analysis revealed correlates in bilateral thalamus, providing support for a thalamo-cortical loop in attentional modulations and suggesting that the cortical alpha rhythm acts as a cyclic modulator of task-related responses very early in the processing stream. Our results help to reconcile the competing inhibition and active-processing hypotheses for ongoing alpha oscillations and begin to tease apart the distinct roles and mechanisms underlying their power and phase.

Keywords

EEG; fMRI; auditory; alpha; phase; attention modulation

1 Introduction

Electroencephalographic (EEG) power in the alpha band (8–12 Hz) is commonly associated with endogenous attention, with high power generally thought to represent a less-attentive idling state of the cortex from which it is measured. While this alpha rhythm is present in many distinct cortical and subcortical regions (Klimesch, 1999), occipito-parietal alpha

*Corresponding Author: psajda@columbia.edu. phone: +1-212-854-5279. mailing address: Columbia University, 351 Engineering Terrace, MC8904, 530 W. 120th St., New York, NY, USA 10027.

activity is the most commonly studied, mainly due to its dominance in scalp EEG recordings (Klimesch, 1999). For example an inverse relationship between occipital-parietal (posterior) alpha power and visual attention has been demonstrated in baseline (prestimulus) activity as well as in responses to stimuli (Klimesch et al., 1998; Makeig et al., 2002; Min & Park, 2010; van Dijk et al., 2008). Extensive evidence shows that the power of alpha oscillations prior to a stimulus correlates negatively with behavioral performance related to visual perceptual ability (Hanslmayr et al., 2007; Mazaheri et al., 2009; van Dijk et al., 2008) while others have shown a similar correlation with visuo-spatial attention (Kelly et al., 2009; Thut et al., 2006).

Less work has been done relating alpha oscillations to auditory task processing. One reason is that ongoing alpha-band oscillations in the primary auditory cortices of the temporal lobes (typically measured using magneto-encephalography (MEG) and referred to as the tau rhythm (Hari et al., 1997; Lehtela et al., 1997)) are difficult to measure with scalp EEG and less prevalent among subjects than the occipito-parietal alpha rhythm (Bastiaansen et al., 2001). However, in addition to its common association with visual attention, posterior alpha activity has been related to audio-spatial attention (Kerlin et al., 2010) and multi-sensory attention (Banerjee et al., 2011; Lange et al., 2013). Furthermore, a number of previous studies have shown an *increase* in posterior alpha power in preparation for expected auditory stimuli (Foxe et al., 1998; Foxe & Snyder, 2011; Fu et al., 2001), suggesting that in the auditory domain the high posterior alpha condition is marking a more engaged state.

In easy tasks with near-perfect performance, variability in the EEG response, instead of task performance, can be related to baseline alpha fluctuations (Barry et al., 2000). Amplitudes of these evoked responses have been shown to be modulated by alpha power (Lou et al., 2014; Rajagovindan & Ding, 2011), but evidence suggests the phase of alpha at stimulus onset may have a greater effect on evoked responses (Fellinger et al., 2011; Mathewson et al., 2009). Alpha phase has also been associated with behavioral performance related to visual perception (Dugue et al., 2011; Mathewson et al., 2009), but the brain regions underlying such phase effects are yet to be identified (Palva & Palva, 2011).

Two alternative hypotheses currently exist for the functional significance of alpha oscillations. The inhibition hypothesis defines an inhibitory role to suppress processing of task-irrelevant stimuli thereby optimizing task performance (Jensen & Mazaheri, 2010; Klimesch et al., 2007), whereas the active-processing hypothesis incorporates the concept of phase dynamics and suggests a role in the neural processing of task-relevant stimuli (Mo et al., 2011; Palva & Palva, 2007; von Stein et al., 2000). In particular, Mathewson et al. (2011) proposed that alpha oscillations reflect a pulsed inhibition of neural activity whereby the phase of the oscillation at stimulus onset is crucial for determining the extent of processing. The inhibition and active-processing hypotheses are not necessarily incompatible (Palva & Palva, 2011). Evidence suggests the role of alpha depends upon the specific cortical (or subcortical) region from which the oscillation was measured (Bollimunta et al., 2008; Mo et al., 2011), cortical layer (Bollimunta et al., 2011), sensory modality of task stimuli and directed attention (Mo et al., 2011), relevance of stimuli to task, and eyes-open vs. eyes-closed condition (Mo et al., 2013).

In this paper we focus on the posterior cortical alpha rhythm as it relates to task-relevant stimulus processing in the auditory domain. We use scalp EEG with simultaneously-acquired functional magnetic resonance imaging (fMRI), and treat the blood oxygen level dependent (BOLD) response as a measure of task-related neural processing. We use prestimulus EEG alpha as an index of a subjects' task engagement on each trial, and contrast the BOLD response for the high vs. low alpha power conditions. Additionally, we investigate how the phase of this oscillation at stimulus onset time relates to the BOLD response. In contrast to previous studies, we investigate not just stimulus processing but also task-relevant processing related to perceptual decision making, and we explore these correlates across the whole brain.

2 Materials and Methods

Our EEG-fMRI data collection and preprocessing were previously described in Walz et al. (2013), but we reproduce much of our description here for ease of the reader. We refer the reader to that previous study for evoked EEG responses and their BOLD correlates. This dataset (which includes an analogous visual experiment) is freely available via the OpenfMRI data repository (Poldrack et al., 2013) (https://openfmri.org/dataset/ds000116).

2.1 Auditory Oddball Paradigm

Seventeen healthy human subjects with no psychiatric or neurological disorders performed a classic auditory oddball task with their eyes closed. Fifteen of them were ultimately included in our analysis (see Section 3). This simple and well-studied paradigm left the subjects' minds free to wander while still maintaining near-perfect behavioral performance, so it was ideal for studying naturally occurring endogenous shifts of attention. We used an auditory experiment because posterior EEG alpha power is highly affected by visual stimulus presentation (Klimesch et al., 2007; Makeig et al., 2002). Furthermore, power in this frequency band is higher with the eyes-closed condition made possible by the auditory experiment (Mo et al., 2013), which increased the signal-to-noise ratio (SNR) of the occipital alpha oscillation. This was especially helpful since the ballistocardiogram (BCG) signal contains high power within the alpha band, and no currently-existing method is able to completely remove this artifact. The eyes-closed condition also ensured that we were measuring true spontaneous activity in the absence of visual input (Logothetis et al., 2009).

The 375 (125 per run) total stimuli were presented for 200 ms each with a 2 to 3 s uniformly-distributed variable inter-trial interval (ITI) using E-Prime software (PST, Pittsburgh, PA). Target stimuli were presented randomly among the standard stimuli with probability $\frac{1}{5}$, and the first two stimuli of each run were constrained to be standards. Standard stimuli were a pure 390 Hz tone (chosen to lie within a trough of the scanner sound frequency spectrum), and target stimuli were a broadband "laser gun" sound. Because our study focused on task-related attentional states, subjects were asked to respond to target stimuli using a button press with the right index finger. The stimuli were presented through headphones using a VisuaStim Digital System (Resonance Technology, Northridge, CA), and behavioral responses were acquired using an MR-compatible button response pad. All subjects gave written informed consent following the protocol of the Columbia University Institutional Review Board.

2.2 EEG-fMRI Data Acquisition

We simultaneously and continuously recorded EEG using a custom-built MR-compatible EEG system (Goldman et al., 2009; Sajda et al., 2010), with differential amplifier and bipolar EEG cap. The caps are configured with 36 Ag/AgCl electrodes including left and right mastoids, arranged as 43 bipolar pairs. Bipolar pair leads are twisted to minimize inductive pickup from the magnetic gradient pulses and subject head motion in the main magnetic field. This oversampling of electrodes ensured data from a complete set of electrodes even in instances when discarding noisy channels was necessary. To enable removal of gradient artifacts in our offline preprocessing, we synchronized the 1-kHz-sampled EEG with the scanner clock by sending a transistor-transistor logic (TTL) pulse to a field-programmable gate array (FPGA) card (National Instruments, Austin, TX) at the start of each of 170 functional image acquisitions. All electrode impedances were kept below 20 kΩ, including 10 kΩ resistors built into each electrode for subject safety. A comprehensive description of the hardware, along with many of the preprocessing and analysis methods described throughout the remainder of this section, can be found in Sajda et al. (2010).

A 3T Philips Achieva MRI scanner (Philips Medical Systems, Bothell, WA) was used to collect functional echo-planar image (EPI) data continuously with 3 mm in-plane resolution and 4 mm slice thickness. We acquired 32 slices of 64 × 64 voxels using a 2000 ms repetition time (TR) and 25 ms echo time (TE). We also acquired a single-volume high resolution (2 × 2 × 2 mm) EPI image and a 1 × 1 × 1 mm spoiled gradient recalled (SPGR) image for each subject for purposes of registration.

2.3 EEG Data Preprocessing

We performed all EEG preprocessing offline using Matlab (Mathworks, Natick, MA). In addition to standard EEG artifacts, EEG signals recorded inside the MRI scanner are contaminated with gradient and BCG pulse artifacts due to magnetic induction in the EEG wires. First we removed the gradient artifacts by subtracting the mean artifact across all functional volume acquisitions. We then applied a 10 ms median filter to remove any residual spike artifacts. Next we removed standard EEG artifacts, using the following digital Butterworth filters: 1 Hz high pass to remove DC drift, 60 Hz and 120 Hz notches to remove electrical line noise and its first harmonic, and 100 Hz low pass to remove high frequency artifacts not associated with neurophysiological processes. These filters were applied together in the form of a linear phase finite impulse response (FIR) filter to avoid distortions caused by phase delays.

BCG artifacts are more challenging to remove, since they both share frequency content with EEG activity and vary from heart beat to heart beat. Currently-existing BCG removal algorithms cause loss of signal power in the underlying EEG, so we performed our alpha estimation (Section 2.4) on the data without BCG artifact removal. This was justified because we made sure to select alpha components that were orthogonal to BCG. However, for the sole purpose of viewing scalp topographies of the independent components, we removed BCG artifacts from the continuous gradient-free data using a principal components analysis (PCA) method (Goldman et al., 2009; Sajda et al., 2010). First we low-pass filtered the data at 4 Hz to extract the signal within the frequency range where BCG artifacts are

observed, and then the first two principal components were determined. The channel weightings corresponding to those components were projected onto the broadband data and subtracted out. We then re-referenced these BCG-free data from the 43 bipolar channels to the 34-electrode space to calculate scalp topographies of the independent components. The final reference in this EEG electrode space was the average of the left and right mastoid signals.

2.4 Prestimulus EEG Alpha Estimation

To determine a projection of the multi-dimensional EEG data containing the alpha activity of interest, we first performed an independent component analysis (ICA) using the FastICA algorithm (Hyvarinen, 1999) in Matlab. This method was chosen over individual electrode selection to increase the SNR of the EEG signal. It was necessary to select a single component because one of our goals was to investigate phase effects. Note however that when we initially ran our alpha power analysis using the mean power across five top-ranked alpha components, results were nearly identical as those described in Sections 3.1 and 3.2.

Figure 1 shows a diagram of the remainder of our methods, which are described below. We selected a single “alpha component” based on three main criteria: (1) high alpha power, in particular relative to surrounding frequency bands, (2) no peak in the 1 Hz range, which would indicate a contaminant from the BCG pulsation artifact, and (3) typical posterior scalp distribution. Evaluation of these selection criteria involved the following. To each component’s time series we applied a 2^{nd} order zero-phase non-causal Butterworth bandpass filter with cutoffs at 8 and 12 Hz, and then estimated the mean power in the alpha band by squaring and summing the resulting signal. We assessed our filter responses to ensure that stimulus-evoked EEG responses were not confounding our estimations of pre-stimulus power or phase (i.e. we checked that the temporal integration of the non-causal filter was only a few milliseconds). We estimated the mean broadband EEG power of each component similarly, using cutoff frequencies at 5 and 20 Hz. Next we calculated the ratio of mean alpha power to mean broadband power for each component, and ranked the components according to this ratio. Spatial topographies of the top five components were displayed to manually select the alpha component with typical posterior distribution, i.e. heavy weighting on occipito-parietal electrodes.

We took care to ensure that the selected component was not contaminated with BCG artifacts. The top five ranked “BCG components” were chosen using a similar method to that just described for selecting the alpha component, but using a 0.5–2 Hz pass band. These components had heavy lateralized weighting on the electrodes, which we expected since temporal electrodes (sites T7, T8, CP5, CP6) are most strongly affected by such pulsation artifacts.

Once the final alpha component was confirmed, we re-centered the pass band of our filter around the subject-specific peak alpha frequency (i.e. cutoffs at ±2 Hz around the subject-specific peak). This modal frequency was selected by visual inspection of the power spectrum of the unfiltered alpha component, and ranged across subjects from 9.5–12 Hz with median of 10.5 Hz. We repeated the alpha band-pass filtering of the original alpha component with this adjusted filter to more accurately extract the alpha activity.

We computed the Hilbert transform of this band-passed alpha component to decompose the alpha oscillation into its magnitude envelope and instantaneous phase across the entire run of the experiment. By visual inspection we discarded trials containing excessive motion artifacts in the EEG data, evidenced by sudden high-amplitude deflections, and also those with incorrect responses (> 95% of trials remained).

In preparation for our pre-stimulus alpha power fMRI analysis, for each trial we computed the mean alpha envelope in the half second prior to stimulus onset (i.e. −500–0 ms relative to stimulus onset), and within each of the two stimulus classes (independently for each subject) we binned trials according to high, medium, or low prestimulus alpha magnitude. Since the magnitude of this envelope is related to the instantaneous power by a constant, we refer to this measurement as power for consistency with the literature.

The phase analysis was run completely independently of the power analysis. For this we divided trials into four groups according to their instantaneous phase at stimulus onset time, as was done previously by Scheeringa et al. (2011) and Barry et al. (2004). This was equivalent to categorizing based on the alpha oscillation's sign (positive or negative), derivative (increasing or decreasing), and direction of deviation from zero (waxing or waning), giving the following four groups:

- 0 to $\frac{\pi}{2}$ – positive, waxing, increasing
- $\frac{\pi}{2}$ to π – positive, waning, decreasing
- π to $\frac{3\pi}{2}$ – negative, waxing, decreasing
- $\frac{3\pi}{2}$ to 2π – negative, waning, increasing

2.5 fMRI Data Preprocessing and Traditional Analysis

Using FSL (Smith et al., 2004), we performed bias-field correction on all images to adjust for artifacts caused by the EEG wires. We then performed slice-timing correction, motion correction, 0.01 Hz high-pass filtering, and 5 mm full width half max (FWHM) spatial smoothing on the functional data. Motion correction provided motion parameters that were later included as confounds in the general linear model (GLM). Functional and structural images were registered to a standard Montreal Neurological Institute (MNI) brain template following brain extraction, and each subject's registration was checked manually to ensure proper alignment.

We first ran a traditional event-related fMRI analysis, using stimulus presentation time and reaction time (RT) variability regressors in our GLM. The stimulus regressors were comprised of boxcar functions with unit amplitude and onset and offset matching that of the stimuli. RT variability was modeled using unit amplitude boxcars with onset at stimulus time and offset at response time, and these were orthogonalized to the stimulus regressors. All regressors were convolved with the canonical hemodynamic response function (HRF), and temporal derivatives were included as confounds of no interest. A target vs. standard contrast was also constructed. A fixed effects model was used to model activations across runs, and a mixed effects approach used to compute the contrasts across subjects. Statistical

image results for these traditional analyses were thresholded at $z > 2.3$, and clusters were multiple-comparison-corrected at $p = 0.05$ (Worsley, 2001).

2.6 EEG Alpha Oscillations and BOLD Response to Auditory Target Stimuli

The fMRI model for the EEG alpha investigation of this study (illustrated in Figure 1D and 1E) differed from the traditional event-related analysis in two ways. Firstly, RT variability was not incorporated into the model but instead included as a nuisance regressor. Secondly and key to this study, trials were binned based on their alpha activity (refer to Section 2.4 and Figure 1) and each bin modeled in separate regressors. The alpha power and alpha phase analyses were performed independently, involving three and four bins of trials, respectively. We computed a high vs. low alpha power contrast within the target class to observe the effect of prestimulus alpha power on the BOLD response to identical target stimuli. We investigated phase effects similarly by contrasting positive vs. negative, waxing vs. waning, and increasing vs. decreasing phase at stimulus onset.

2.7 EEG Alpha Oscillations and Decision-Related BOLD Activity

Scheeringa et al. (2011) suggested that a correlation between the underlying BOLD signal and slow alpha fluctuations could confound the analysis described above (high power vs. low power contrast), so we also investigated the effect of prestimulus alpha oscillations on processing related to the decision making task. For both the high alpha and low alpha trial groups we computed target vs. standard contrasts to reveal the most task-relevant fMRI activity. This approach effectively subtracted out the BOLD correlates of baseline alpha power and isolated BOLD activity related to post-stimulus processing.

For both the high alpha and low alpha trial groups we computed target vs. standard contrasts to reveal the most task-relevant fMRI activity. This approach effectively subtracted out the BOLD correlates of baseline alpha power and isolated BOLD activity related to post-stimulus processing. Even in our simple task, the resulting activations included areas involved in early auditory processing, target detection, perceptual decision making, a go/no-go response decision and planning, and motor processing. We then performed a paired t-test high alpha power vs. low alpha power on the individual subjects' results to identify effects of prestimulus alpha power on the task-relevant BOLD activity.

Although the phase analysis was not confounded by any intrinsic correlation between underlying alpha power fluctuations, we performed the same task-related processing investigation as we did for alpha power. We similarly grouped trials (this time into the four phase bins: positive waxing increasing, positive waning decreasing, negative waxing decreasing, negative waning increasing), and contrasted target vs. standard BOLD responses within each of these four groups. We performed three paired t-tests of these contrasts: positive vs. negative (i.e. peak vs trough), increasing vs. decreasing (i.e. growing more positive or more negative), and waxing vs. waning (i.e. alpha oscillation moving away from zero vs. toward zero).

2.8 Statistical Thresholding Procedure

We thresholded the group level fMRI statistical maps at per-voxel $p < 0.005$ then cluster-corrected them at $p < 0.05$ using a randomization method to generate a null distribution of clusters. For each subject, we randomly grouped trials 100 times and for each randomization ran the fMRI analysis described above. We created 500 group-level statistical maps by carrying random samplings of the subject-level results to the group level (Stelzer et al., 2013), both for the target response analysis and the paired t-test analysis. Each of these group-level randomization maps were thresholded at per-voxel $p < 0.005$ to provide a null distribution of clusters. Within each of these clusters we summed the negative log of each voxel's p-value to create a null distribution of cluster p-values, from which we calculated the $p < 0.05$ cluster threshold. This method of integrating statistics within each cluster is closely related to a cluster size thresholding, but gives a higher weighting to clusters with stronger voxel-wise statistical strength. These randomizations were run independently for each of the analyses described in Sections 2.6 and 2.7 to generate distributions specific to each of them. The four resulting distributions were comprised of 10562 ± 1538 clusters, and the cluster size roughly corresponding to $p = 0.05$ was 24 ± 2 voxels.

3 Results

Data from two of the seventeen subjects were discarded due to a slow EEG alpha power drift across the entire experiment that left us with an incomplete fMRI model (i.e. empty regressors) for some runs of the experiment. This was not an issue for the phase analysis since our ITI was jittered and the phase at stimulus onset was uniformly distributed as a result; however, for consistency we used the same group of fifteen subjects in both the power and phase analyses. Demographics of these fifteen remaining subjects were: 6 female, mean 27.5 years, range 20–40. All fifteen included subjects responded with high accuracy and speed: $98.8\% \pm 2.1\%$ of targets were correctly detected, with 403.0 ± 60.1 ms RT. We did not detect any significant correlation between RT and pre-stimulus alpha power, which is not unexpected since attentional fluctuations do not affect behavioral responses during such an easy task.

The mean BOLD response to target stimuli was consistent with previous findings (Stevens et al., 2000), showing the largest positive activations in thalamus, auditory cortex, insular cortex, and contralateral supplementary and primary motor areas, and showing the largest negative activations in visual areas and ipsilateral motor areas (Figure 2). As expected, the target vs. standard contrast showed even stronger and more widespread activations (Figure 3). For fair interpretation of the results that were the focus of this study (described in the sections that follow), we confirmed that all significant activations in the separate high prestimulus alpha and low prestimulus alpha contrasts matched sign in corresponding brain regions. BOLD correlates of RT variability are provided in Supplementary Figure 2. The mean scalp topography of the EEG alpha components across the 15 subjects is shown in Supplementary Figure 1. A typical posterior distribution was clearly seen, without any visible contribution from BCG artifact, which would have been evident from a bilateral weighting at temporal sites.

3.1 Effect of Prestimulus Alpha Power on BOLD Response to Auditory Target Stimuli

Negative correlation between the BOLD signal and prestimulus alpha power was found throughout posterior regions for the high vs. low alpha contrast of the response to target stimuli (Figure 4). These regions included left and right lateral occipital cortices (LOC) and lingual gyri, as well as left precuneus and occipital pole. We also found a positive correlate in the left cerebellum. A complete list of activations exceeding the cluster-corrected $p < 0.05$ threshold can be found in Table 1.

3.2 Effect of Prestimulus Alpha Power on Decision-Related Processing

We found a greater difference in the positive BOLD response to targets as compared to standards (i.e. target vs. standard contrast) in cingulate and contralateral motor areas for the high alpha condition as compared to the low alpha condition (Figure 5). These activations were strong and widespread, covering 253 voxels ($p_{cluster} = 0.0003$) in the cingulate and 104 voxels ($p_{cluster} = 0.0028$) in left postcentral gyrus. These clusters both corresponded to areas of positive BOLD activation in the target vs. standard contrast of the traditional analysis, and more specifically a stronger positive BOLD response to targets compared to standards for all trials regardless of alpha activity). Ipsilateral motor areas were also activated, but not quite as extensively, and these corresponded to areas with negative activation in the traditional target vs. standard contrast, and more specifically a stronger negative BOLD response to targets as compared to standards. We also found symmetric bilateral activations in precentral, postcentral, and middle frontal gyri. A complete list of all clusters exceeding the $p < 0.05$ threshold can be found in the bottom half of Table 1.

3.3 Effect of Alpha Phase on BOLD Response to Auditory Target Stimuli

We also found supra-threshold fMRI correlates of the alpha oscillation's phase at stimulus onset (Table 2). The positive vs. negative phase contrast resulted in a positive activation in right precuneus as well as negative correlates in left and right thalamus (Figure 6). The increasing vs. decreasing phase contrast resulted in a negative BOLD correlate in the left middle frontal gyrus. The thalamic clusters corresponded to a positive BOLD response in the traditional analysis results, and the precuneus corresponded to a negative BOLD response.

3.4 Effect of Alpha Phase on Decision-Related Processing

Table 2 (bottom half) contains a list of all clusters exceeding the $p < 0.05$ cluster threshold for the alpha phase paired t-tests of the target vs. standard contrast. For the paired t-test of waxing vs. waning phase we found positive correlates in precuneus, frontal pole, left occipital pole, and right superior LOC. The positive vs. negative phase t-test (i.e. peak vs. trough) revealed large negative correlates in bilateral thalamus (118 voxels for left and 61 for right, Figure 7). The increasing vs. decreasing t-test resulted in a positive correlate in right hippocampus and negative correlates in left middle frontal gyrus. Again, the thalamic clusters corresponded to a positive BOLD result in the traditional contrast (i.e. stronger positive activation in thalamus for targets compared to standards.

4 Discussion

In the context of the EEG-fMRI literature investigating prestimulus EEG alpha affects on the BOLD response during a task, our study is novel in four ways: (1) we explored the whole brain instead of just ROIs, (2) we investigated stimulus processing in the auditory domain, (3) we explored task-relevant stimulus processing (as opposed to distractor stimuli that were unrelated to the task), and (4) we investigated decision-related processing by contrasting the target vs. standard BOLD responses. Furthermore, only one previous published study (Scheeringa et al., 2011) has investigated how the phase of the alpha oscillation at stimulus onset correlates with the BOLD response.

4.1 Prestimulus Alpha Power Correlates with BOLD Activity Related to Auditory Perceptual Decision Process

We found an inverse correlation between prestimulus EEG alpha power and the BOLD response throughout occipital areas and a positive correlate in the cerebellum (Table 1), consistent with resting-state findings (Goldman et al., 2002; Liu et al., 2012; Mantini et al., 2007). Similar results have also been reported for visual tasks (Becker et al., 2011; Mayhew et al., 2013), but Scheeringa et al. (2011) found no significant effect of prestimulus alpha power on the BOLD response after accounting for ongoing alpha-BOLD correlations. Scheeringa et al. removed this confound by subtracting the mean “pseudo trial” response (no stimulus) from the mean “real trial” time courses within visual ROIs. Given our binary decision making task with short (2–3 s) ITI between stimuli, we needed to address this potential confound differently. By first contrasting the BOLD response to target vs. standard stimuli separately for each prestimulus alpha power group (high, medium, low), we remove this confound while also focusing on higher-level processing. Significant activations for this analysis reveal the brain regions involved in the perceptual decision making process, along with motor planning and behavioral performance monitoring. We then performed a paired t-test of these target vs. standard contrasts for the high vs. low prestimulus alpha conditions to reveal the effect of alpha power on task-related processing.

We found the largest differences in the supplementary motor area (SMA) of the cingulate cortex (253 voxel cluster at a $p < 0.005$ per voxel threshold) and contralateral motor areas, though pre-central and post-central gyri were activated bilaterally. These motor area activations are not an effect of RT variability, since RT was not correlated with prestimulus EEG alpha power and we included RT as a nuisance regressor. All of our activations resulting from the high vs. low alpha power t-test were positive in sign. Since posterior alpha power has been shown to increase as subjects focus attention toward upcoming auditory stimuli (Foxe et al., 1998; Foxe & Snyder, 2011; Fu et al., 2001), we interpret our result as a stronger decision-related response when the subject is more engaged in the auditory task prior to the stimulus. More specifically, the large activations in motor areas may represent increased awareness of the behavioral response. Further, the stronger negative BOLD responses in ipsilateral motor areas demonstrate greater suppression of the ipsilateral motor areas during the focused state, pulling resources toward the contralateral regions required for the behavioral response. Since frontal regions are most commonly associated with effortful decision making related to difficulty (Heekeren et al., 2008; Philiastides &

Sajda, 2007), our increased activations in right inferior frontal gyrus (IFG) and bilateral middle frontal gyri (MFG) may represent greater effort during periods of high task engagement. This finding shows that the likely mechanism by which focused attention leads to optimized performance is through strengthening task-related neural processing, including both increased recruitment of areas directly related to decision processing and increased task-related suppression of areas not directly related to the decision process.

Another interpretation involves the idea of a push-pull effect of attentional allocation and preparedness between sensory input modalities. Several studies have found that cueing attention toward upcoming auditory stimuli resulted in increased occipito-parietal alpha power (Foxe et al., 1998; Foxe & Snyder, 2011; Fu et al., 2001), and a similar effect of increased posterior alpha with somatosensory attention was reported in Anderson & Ding (2011). Fu et al. (2001) localized this alpha rhythm to inferior parietal regions and suggested their role in deployment of attention. In our paradigm, subjects were instructed to attend only to the auditory task while keeping their eyes closed, so it is doubtful that attention would drift toward anticipation of visual input. If here we are indeed observing a push-pull effect of alpha power between sensory cortices, it is likely one that is physiologically hard-wired into the human brain.

Regardless of the choice of interpretation, our results are consistent with the idea of an excitation-inhibition tuning role for the alpha rhythms generated in sensory cortices (Weisz et al., 2011), and in particular a positive relationship between the strength of alpha and processing in higher areas. Our bilateral activations (see Figure 5), particularly those in frontal regions traditionally associated with executive processing, suggest that alpha power modulates decision-related activity significantly downstream from sensory processing. The hypothesized active-processing role of alpha suggests such an effect for task-relevant stimulus processing in higher regions (see Section 4.3). Altogether, top-down alpha power modulations appear to be most important for natural environments full of extraneous sensory information. Their purpose likely includes task-related suppression to better focus attention to the behaviorally-relevant sensory modality in order to optimize performance in the presence of sensory clutter. This is in line with the recent MEG findings of Mazaheri et al. (2014), who showed that top-down alpha power modulations affect behavioral performance only in the presence of a distractor stimulus of another modality.

4.2 Support for thalamo-cortical loop in functional role of cortical alpha rhythm

We show that the phase of the alpha oscillation at stimulus onset affects the BOLD response related to task-relevant stimulus processing. Though difficult to interpret the phase itself (Qian & Xin, 2011), we see thalamus recruited more strongly when the alpha oscillation is in one phase (peak/positive amplitude) vs. the opposite phase (trough/negative amplitude). In the case of stimuli presented in the trough of the alpha wave, cortical regions not directly involved in auditory task processing, such as the right precuneus, are suppressed more strongly than in the peak phase condition. Scheeringa et al. (2011), whose focus was task-irrelevant visual stimulus processing within visual cortex, found that the BOLD response in Brodmann areas 17 and 18 was significantly greater when stimuli were presented during the trough vs. the peak of the alpha oscillation. We did not detect any supra-threshold (cluster

corrected $p < 0.05$) effect in that area, suggesting that the effect of phase on stimulus processing is dependent on sensory input modality and/or relevance of stimulus to task.

We similarly found that decision-related BOLD activity in bilateral thalamic regions was stronger when the stimulus was presented during the trough vs. the peak of the alpha wave. The specific location appears to be the medial dorsal nuclei, which is consistent with a resting state study (Liu et al., 2012) that aimed to link cortical alpha to specific regions of the nuclei. However, given the resolution of our functional images we cannot identify specific nuclei with certainty. Regardless, this finding strongly supports the idea of a thalamo-cortical loop related to the alpha rhythm. Note that we are not studying the alpha rhythm within the thalamus, which can be present independently of or in synchrony with cortical alpha oscillations (Lopes da Silva et al., 1980). Instead we are measuring cortical alpha oscillations and observing an effect of phase on task-related thalamic BOLD responses. The thalamus has been shown to be a key region in coordinating cortical alpha oscillations (Hughes & Crunelli, 2007), and our results suggest a more complex interaction. It is possible that cortical alpha activity and thalamic activity actually share a common modulator, or cortical alpha might feed back to directly modulate activity in the thalamus. This ambiguity should be resolved using animal models or with EEG in combination with transcranial magnetic stimulation (TMS).

4.3 Insight into the functional roles of alpha power and phase

We show that prestimulus power and phase of the posterior alpha oscillation differently influence task-relevant auditory stimulus processing. Our results show that prestimulus alpha power has a modulatory role (gain effect) that boosts higher-level processing related to task performance (e.g. performance monitoring) but does not show this gain effect in primary sensory areas, at least not for our easy auditory perceptual decision making task. These findings are consistent with the idea that the functional role of alpha and its underlying mechanisms vary along the cortical processing stream (Bollimunta et al., 2008, 2011; Palva & Palva, 2011).

We found that alpha phase most strongly influences evoked task-related BOLD activity in the thalamus when the stimulus is presented in the alpha trough vs. peak. Since the thalamus is a major relay center early in the stimulus processing stream, such a modulation might serve as a mechanism of gain in higher level areas. More broadly, the phase effects we detected support the idea that alpha oscillations reflect cyclic modulations of neuronal excitability (Mathewson et al., 2011; Palva & Palva, 2011). Mathewson et al. (2011) proposed that peaks and troughs of the alpha wave at stimulus onset act as a pulsed inhibition of continuous visual processing. Our results extend this idea to include auditory tasks, showing that the alpha rhythm in posterior areas (which are not thought to be directly related to auditory tasks) can affect processing related to auditory perceptual decision making. This adds to growing evidence showing that alpha acts to route information across the brain to task-relevant cortices via a pulsed gating by inhibition of task-irrelevant cortices (Jensen & Mazaheri, 2010; Klimesch et al., 2007). In a recent MEG study focused on top-down modulations of alpha power in visual and auditory cortices, Mazaheri et al. (2014)

also suggested that the idea of alpha power as cortical information gating can be generalized to the auditory modality.

Our findings support the active processing hypothesis for the role of the alpha rhythm, in which phase dynamics have an effect on coordinating task-relevant neural processing, and we expand upon this to suggest that this mechanism occurs through modulation of thalamic responses. Our results are also in agreement with and even expand upon the inhibition hypothesis, which has most commonly been explored using task-irrelevant distractors. Here we studied only task-relevant processing, and we see an increased task-related suppression of areas not directly related to the task. Follow-up studies should be designed to investigate both task-relevant stimuli as well as background stimuli that act as distractors within one paradigm. With this study, we move toward a deeper understanding of the role of the posterior cortical alpha rhythm in auditory task-related processing occurring across the entire brain and help to reconcile the competing inhibition and active-processing hypotheses.

Supplementary Material

Refer to Web version on PubMed Central for supplementary material.

Acknowledgments

This work was funded by National Institutes of Health Grant R01-MH085092 and by the National Science Foundation Graduate Research Fellowship Program. We thank Glenn Castillo and Stephen Dashnaw for their assistance with EEG-fMRI data acquisition.

References

Anderson KL, Ding M. Attentional modulation of the somatosensory mu rhythm. J Neurosci. 2011; 180:165–180.

Banerjee S, Snyder AC, Molholm S, Foxe JJ. Oscillatory alpha-band mechanisms and the deployment of spatial attention to anticipated auditory and visual target locations: supramodal or sensory-specific control mechanisms? J Neurosci. 2011; 31(27):9923–9932. [PubMed: 21734284]

Barry RJ, Kirkaikul S, Hodder D. EEG alpha activity and the ERP to target stimuli in an auditory oddball paradigm. Int J Psychophysiol. 2000; 39(1):39–50. [PubMed: 11120346]

Barry RJ, Rushby JA, Johnstone SJ, Clarke AR, Croft RJ, Lawrence CA. Event-related potentials in the auditory oddball as a function of EEG alpha phase at stimulus onset. Clin Neurophysiol. 2004; 115(11):2593–601. [PubMed: 15465449]

Bastiaansen MC, Bocker KB, Brunia CH, de Munck JC, Spekreijse H. Event-related desynchronization during anticipatory attention for an upcoming stimulus: a comparative EEG/meg study. Clin Neurophysiol. 2001; 112(2):393–403. [PubMed: 11165546]

Becker R, Reinacher M, Freyer F, Villringer A, Ritter P. How ongoing neuronal oscillations account for evoked fMRI variability. J Neurosci. 2011; 31(30):11016–27. [PubMed: 21795550]

Bollimunta A, Chen Y, Schroeder CE, Ding M. Neuronal mechanisms of cortical alpha oscillations in awake-behaving macaques. J Neurosci. 2008; 28(40):9976–88. [PubMed: 18829955]

Bollimunta A, Mo J, Schroeder CE, Ding M. Neuronal mechanisms and attentional modulation of corticothalamic alpha oscillations. J Neurosci. 2011; 31(13):4935–43. [PubMed: 21451032]

Dugue L, Marque P, VanRullen R. The phase of ongoing oscillations mediates the causal relation between brain excitation and visual perception. J Neurosci. 2011; 31(33):11889–93. [PubMed: 21849549]

Fellinger R, Klimesch W, Gruber W, Freunberger R, Doppelmayr M. Pre-stimulus alpha phase-alignment predicts P1-amplitude. Brain Res Bull. 2011; 85(6):417–23. [PubMed: 21473900]

Foxe JJ, Simpson GV, Ahlfors SP. Parieto-occipital approximately 10 hz activity reflects anticipatory state of visual attention mechanisms. Neuroreport. 1998; 9(17):3929–33. [PubMed: 9875731]

Foxe JJ, Snyder AC. The role of alpha-band brain oscillations as a sensory suppression mechanism during selective attention. Frontiers in psychology. 2011; 2(54):1–13. [PubMed: 21713130]

Fu KMG, Foxe JJ, Murray MM, Higgins BA, Javitt DC, Schroeder CE. Attention-dependent suppression of distractor visual input can be cross-modally cued as indexed by anticipatory parieto-occipital alpha-band oscillations. Cogn Brain Res. 2001; 12:145–152.

Goldman RI, Stern JM, Engel JJ, Cohen MS. Simultaneous EEG and fMRI of the alpha rhythm. Neuroreport. 2002; 13:2487–92. [PubMed: 12499854]

Goldman RI, Wei CY, Philiastides MG, Gerson AD, Friedman D, Brown TR, Sajda P. Single-trial discrimination for integrating simultaneous EEG and fMRI: identifying cortical areas contributing to trial-to-trial variability in the auditory oddball task. Neuroimage. 2009; 47:136–47. [PubMed: 19345734]

Hanslmayr S, Aslan A, Staudigl T, Klimesch W, Herrmann CS, Bauml KH. Prestimulus oscillations predict visual perception performance between and within subjects. Neuroimage. 2007; 37(4): 1465–73. [PubMed: 17706433]

Hari R, Salmelin R, Makela JP, Salenius S, Helle M. Magnetoencephalographic cortical rhythms. Int J Psychophysiol. 1997; 26(1–3):51–62. [PubMed: 9202994]

Heekeren HR, Marrett S, Ungerleider LG. The neural systems that mediate human perceptual decision making. Nature reviews. Neuroscience. 2008; 9(6):467–79. [PubMed: 18464792]

Hughes SW, Crunelli V. Just a phase they're going through: the complex interaction of intrinsic high-threshold bursting and gap junctions in the generation of thalamic alpha and theta rhythms. Int J Psychophysiol. 2007; 64(1):3–17. [PubMed: 17000018]

Hyvarinen A. Fast and robust fixed-point algorithms for independent component analysis. IEEE Trans Neural Netw. 1999; 10(3):626–34. [PubMed: 18252563]

Jensen O, Mazaheri A. Shaping functional architecture by oscillatory alpha activity: gating by inhibition. Front Hum Neurosci. 2010; 4:186. [PubMed: 21119777]

Kelly SP, Gomez-Ramirez M, Foxe JJ. The strength of anticipatory spatial biasing predicts target discrimination at attended locations: a high-density EEG study. Eur J Neurosci. 2009; 30(11): 2224–34. [PubMed: 19930401]

Kerlin JR, Shahin AJ, Miller LM. Attentional gain control of ongoing cortical speech representations in a "cocktail party". J Neurosci. 2010; 30(2):620–8. [PubMed: 20071526]

Klimesch W. EEG alpha and theta oscillations reflect cognitive and memory performance: a review and analysis. Brain Res Brain Res Rev. 1999; 29(2–3):169–95. [PubMed: 10209231]

Klimesch W, Doppelmayr M, Russegger H, Pachinger T, Schwaiger J. Induced alpha band power changes in the human EEG and attention. Neurosci Lett. 1998; 244(2):73–6. [PubMed: 9572588]

Klimesch W, Sauseng P, Hanslmayr S. EEG alpha oscillations: the inhibition-timing hypothesis. Brain Res Rev. 2007; 53(1):63–88. [PubMed: 16887192]

Lange J, Oostenveld R, Fries P. Reduced occipital alpha power indexes enhanced excitability rather than improved visual perception. J Neurosci. 2013; 33(7):3212–20. [PubMed: 23407974]

Lehtela L, Salmelin R, Hari R. Evidence for reactive magnetic 10-hz rhythm in the human auditory cortex. Neurosci Lett. 1997; 222(2):111–4. [PubMed: 9111741]

Liu Z, de Zwart JA, Yao B, van Gelderen P, Kuo LW, Duyn JH. Finding thalamic BOLD correlates to posterior alpha EEG. Neuroimage. 2012; 63(3):1060–9. [PubMed: 22986355]

Logothetis NK, Murayama Y, Augath M, Steffen T, Werner J, Oeltermann A. How not to study spontaneous activity. Neuroimage. 2009; 45(4):1080–9. [PubMed: 19344685]

Lopes da Silva F, Vos J, Mooibroek J, Van Rotterdam A. Relative contributions of intracortical and thalamo-cortical processes in the generation of alpha rhythms, revealed by partial coherence analysis. Electroencephalogr Clin Neurophysiol. 1980; 50(5–6):449–456. [PubMed: 6160987]

Lou B, Li Y, Philiastides MG, Sajda P. Prestimulus alpha power predicts fidelity of sensory encoding in perceptual decision making. Neuroimage. 2014; 87:242–51. [PubMed: 24185020]

Makeig S, Westerfield M, Jung TP, Enghoff S, Townsend J, Courchesne E, Sejnowski TJ. Dynamic brain sources of visual evoked responses. Science. 2002; 295(5555):690–4. [PubMed: 11809976]

Mantini D, Perrucci MG, Del Gratta C, Romani GL, Corbetta M. Electrophysiological signatures of resting state networks in the human brain. Proc Natl Acad Sci U S A. 2007; 104:13170–5. [PubMed: 17670949]

Mathewson KE, Gratton G, Fabiani M, Beck DM, Ro T. To see or not to see: prestimulus alpha phase predicts visual awareness. J Neurosci. 2009; 29(9):2725–32. [PubMed: 19261866]

Mathewson KE, Lleras A, Beck DM, Fiabiani M, Ro T, Gratton G. Pulsed out of awareness: EEG alpha oscillations represent a pulsed-inhibition of ongoing cortical processing. Frontiers in psychology. 2011; 2(99):1–15. [PubMed: 21713130]

Mayhew SD, Ostwald D, Porcaro C, Bagshaw AP. Spontaneous EEG alpha oscillation interacts with positive and negative BOLD responses in the visual-auditory cortices and default-mode network. Neuroimage. 2013; 76:362–72. [PubMed: 23507378]

Mazaheri A, Nieuwenhuis IL, van Dijk H, Jensen O. Prestimulus alpha and mu activity predicts failure to inhibit motor responses. Hum Brain Mapp. 2009; 30(6):1791–800. [PubMed: 19308934]

Mazaheri A, van Schouwenburg MR, Dimitrijevic A, Denys D, Cools R, Jensen O. Region-specific modulations in oscillatory alpha activity serve to facilitate processing in the visual and auditory modalities. Neuroimage. 2014; 87:356–62. [PubMed: 24188814]

Min BK, Park HJ. Task-related modulation of anterior theta and posterior alpha EEG reflects top-down preparation. BMC Neurosci. 2010; 11:79. [PubMed: 20584297]

Mo J, Liu Y, Huang H, Ding M. Coupling between visual alpha oscillations and default mode activity. Neuroimage. 2013; 68:112–8. [PubMed: 23228510]

Mo J, Schroeder CE, Ding M. Attentional modulation of alpha oscillations in macaque inferotemporal cortex. J Neurosci. 2011; 31(3):878–82. [PubMed: 21248111]

Palva S, Palva JM. New vistas for alpha-frequency band oscillations. Trends Neurosci. 2007; 30(4): 150–8. [PubMed: 17307258]

Palva S, Palva JM. Functional roles of alpha-band phase synchronization in local and large-scale cortical networks. Front Psychol. 2011; 2:204. [PubMed: 21922012]

Philiastides MG, Sajda P. EEG-informed fMRI reveals spatiotemporal characteristics of perceptual decision making. J Neurosci. 2007; 27(48):13082–91. [PubMed: 18045902]

Poldrack RA, Barch DM, Mitchell JP, Wager TD, Wagner AD, Devlin JT, Cumba C, Koyejo O, Milham MP. Toward open sharing of task-based fMRI data: the openfMRI project. Front Neuroinform. 2013; 7:12. [PubMed: 23847528]

Qian C, Xin D. Phase or amplitude? the relationship between ongoing and evoked neural activity. J Neurosci. 2011; 31(29):10425–10426. [PubMed: 21775586]

Rajagovindan R, Ding M. From prestimulus alpha oscillation to visual-evoked response: an inverted-u function and its attentional modulation. J Cogn Neurosci. 2011; 23(6):1379–94. [PubMed: 20459310]

Sajda, P.; Goldman, RI.; Dyrholm, M.; Brown, TR. Chapter 9: Signal Processing and Machine Learning for Single-trial Analysis of Simultaneously Acquired EEG and fMRI. Academic Press; 2010.

Scheeringa R, Mazaheri A, Bojak I, Norris DG, Kleinschmidt A. Modulation of visually evoked cortical fMRI responses by phase of ongoing occipital alpha oscillations. J Neurosci. 2011; 31(10): 3813–20. [PubMed: 21389236]

Smith SM, Jenkinson M, Woolrich MW, Beckmann CF, Behrens TE, Johansen-Berg H, Bannister PR, De Luca M, Drobnjak I, Flitney DE, Niazy RK, Saunders J, Vickers J, Zhang Y, De Stefano N, Brady JM, Matthews PM. Advances in functional and structural mr image analysis and implementation as fsl. Neuroimage. 2004; 23:S208–19. [PubMed: 15501092]

Stelzer J, Chen Y, Turner R. Statistical inference and multiple testing correction in classification-based multi-voxel pattern analysis (mvpa): random permutations and cluster size control. Neuroimage. 2013; 65:69–82. [PubMed: 23041526]

Stevens AA, Skudlarski P, Gatenby JC, Gore JC. Event-related fMRI of auditory and visual oddball tasks. Magn Reson Imaging. 2000; 18:495–502. [PubMed: 10913710]

Thut G, Nietzel A, Brandt SA, Pascual-Leone A. Alpha-band electroencephalographic activity over occipital cortex indexes visuospatial attention bias and predicts visual target detection. J Neurosci. 2006; 26(37):9494–502. [PubMed: 16971533]

van Dijk H, Schoffelen JM, Oostenveld R, Jensen O. Prestimulus oscillatory activity in the alpha band predicts visual discrimination ability. J Neurosci. 2008; 28(8):1816– 23. [PubMed: 18287498]

von Stein A, Chiang C, Konig P. Top-down processing mediated by interareal synchronization. Proc Natl Acad Sci U S A. 2000; 97(26):1474814753.

Walz JM, Goldman RI, Carapezza M, Muraskin J, Brown TR, Sajda P. Simultaneous EEG-fMRI reveals temporal evolution of coupling between supramodal cortical attention networks and the brainstem. J Neurosci. 2013; 33(49):19212–19222. [PubMed: 24305817]

Weisz N, Hartmann T, Muller N, Lorenz I, Obleser J. Alpha rhythms in audition: cognitive and clinical perspectives. Front Psychol. 2011; 2:73. [PubMed: 21687444]

Worsley, KJ. Chapter 14: Statistical Analysis of Activation Images. Oxford University Press; 2001.

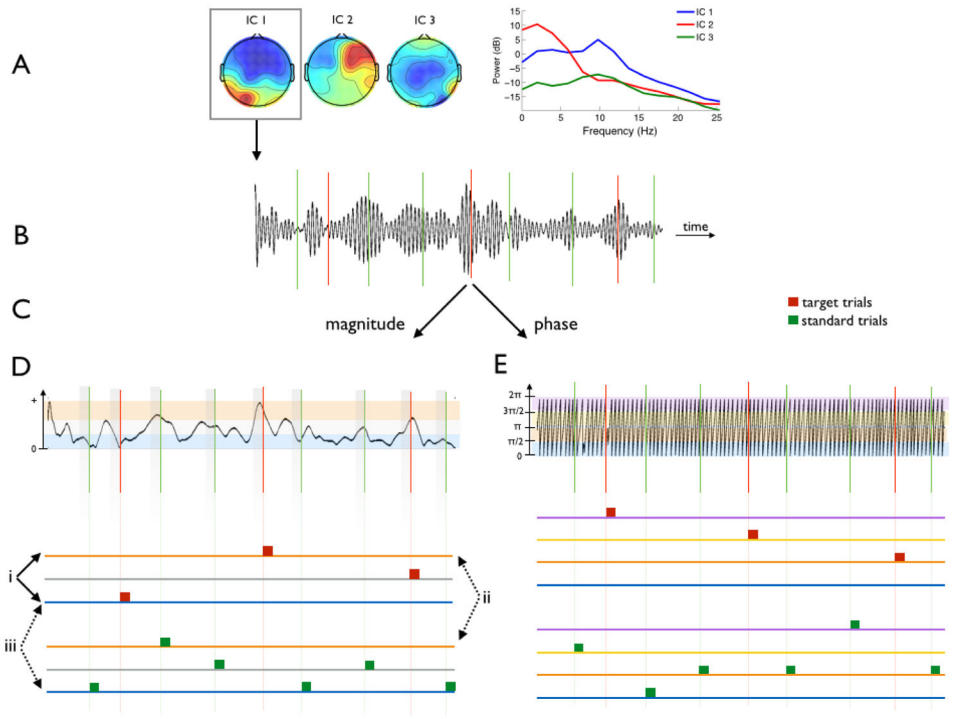

Figure 1. Construction of fMRI Model Based on EEG Alpha Activity

EEG was collected in the fMRI scanner while subjects performed an auditory oddball task. Following preprocessing, ICA was applied to the continuous EEG. **A.** One "alpha component" was selected for all further analyses based on its power spectrum and scalp topography. **B.** The alpha component was bandpass filtered to extract the ongoing alpha activity. **C.** The Hilbert transform decomposed the signal into its magnitude and phase. **D.** Power Analysis BOLD Model: Trials were binned within stimulus class (targets represented in red, standards in green) into 3 groups based on high (orange), medium (grey), or low (blue) prestimulus alpha power. These groups were modeled separately so 3 contrasts (labeled i–iii) could be computed. Contrast i explored the effect of prestimulus alpha power on the target response. A paired t-test between contrasts ii and iii explored the effect of prestimulus alpha power on decision-related processing. **E.** Phase Analysis BOLD Model: Trials were binned into 4 groups according to instantaneous phase of the alpha oscillation at stimulus onset: 0 to $\frac{\pi}{2}$ (blue), $\frac{\pi}{2}$ to π (orange), π to $\frac{3\pi}{2}$ (yellow), and $\frac{3\pi}{2}$ to 2π (purple). Similar contrasts were performed here and are described within the text. Real data is shown, but ITI was shortened here relative to the alpha oscillation for illustration purposes.

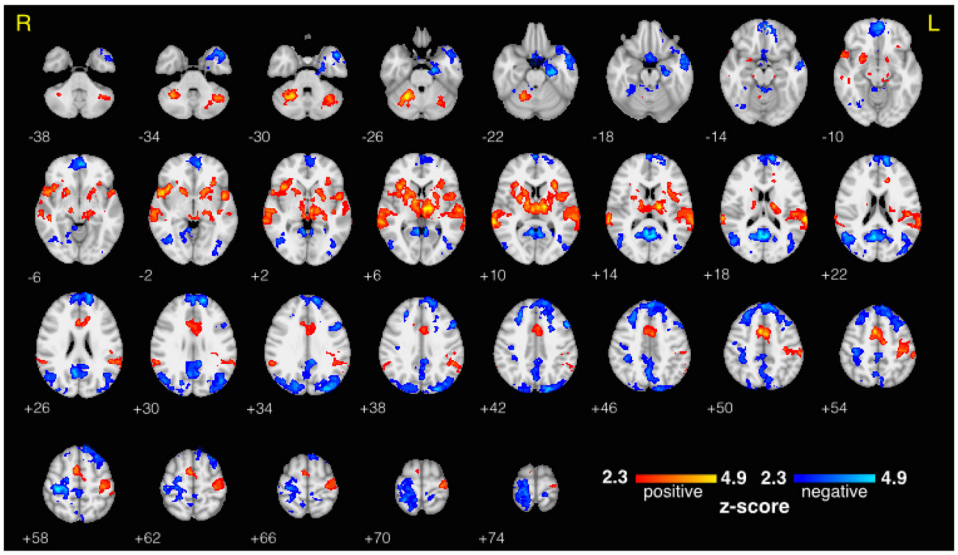

Figure 2. Traditional fMRI Results - Average BOLD Response to Target Trials

Group level average fMRI BOLD response to auditory target stimuli (including all trials regardless of alpha activity), thresholded at $z > 2.3$ and cluster corrected at $p < 0.05$. Statistical maps are displayed on an MNI template brain using radiological coordinates, and z-coordinate is displayed to the lower left of each axial slice.

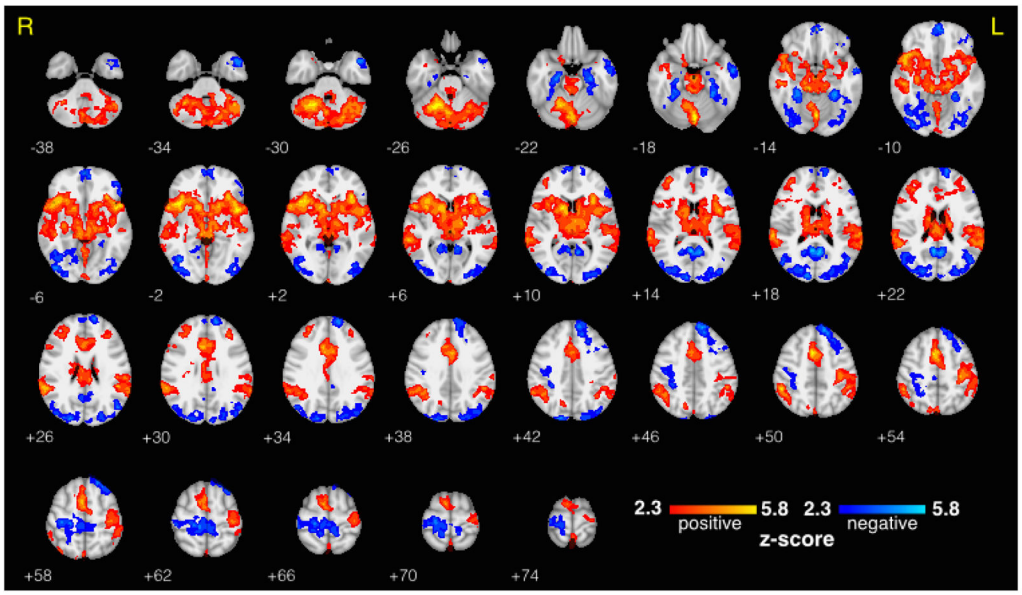

Figure 3. Traditional fMRI Results - Target vs. Standard Contrast

Group level target vs. standard BOLD fMRI contrast (including all trials regardless of alpha activity), thresholded at $z > 2.3$ and cluster corrected at $p < 0.05$. Statistical maps are displayed on an MNI template brain using radiological coordinates, and z-coordinate is displayed to the lower left of each axial slice.

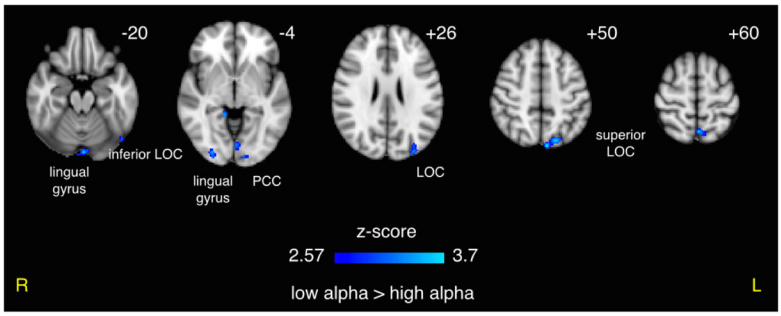

Figure 4. Effect of Prestimulus Alpha Power on BOLD Response to Auditory Targets

An inverse correlation between prestimulus alpha power and the BOLD response was seen throughout many posterior regions, suggesting a possible confound with underlying alpha-BOLD coupling. Results shown were per-voxel thresholded at $p < 0.005$ then cluster-thresholded at $p < 0.05$ and are displayed in radiological orientation on an MNI template brain. z coordinates are specified.

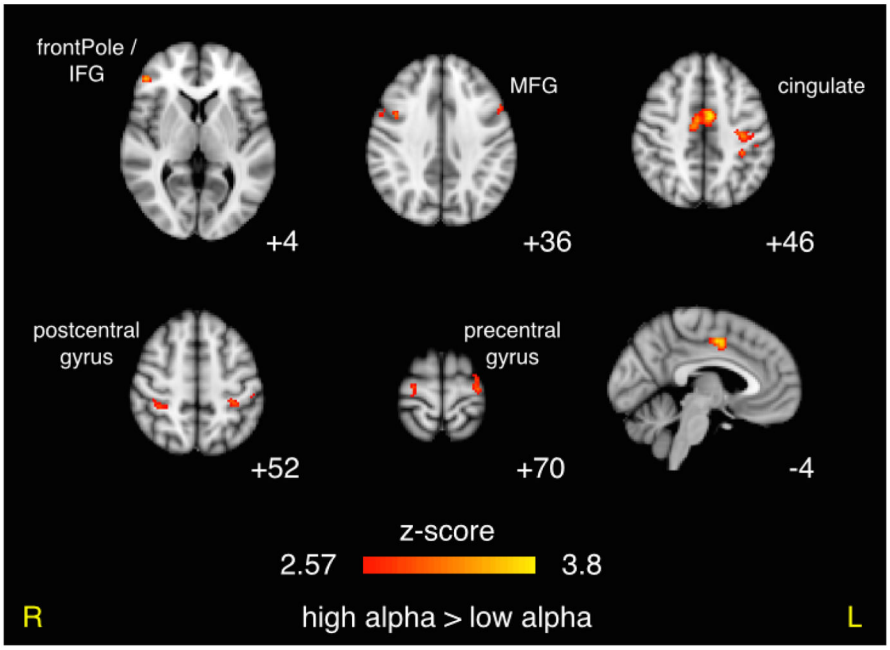

Figure 5. Effect of Prestimulus Alpha Power on Decision-Related BOLD Activity

Results of paired t-test comparing the target vs. standard contrasts for high vs. low alpha power prior to stimulus. Results shown were per-voxel thresholded at $p < 0.005$ then cluster-thresholded at $p < 0.05$ and are displayed in radiological orientation on an MNI template brain. z coordinates are specified for the axial images and y coordinate is specified for the sagittal image.

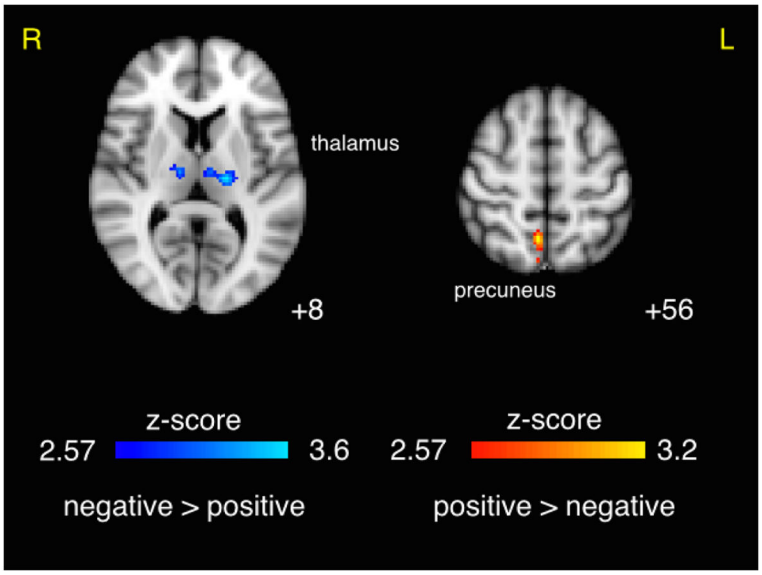

Figure 6. Effect of Prestimulus Alpha Phase on BOLD Response to Auditory Targets

Contrasts showing BOLD response to target stimuli for negative vs. positive (trough vs. peak) and positive vs. negative (peak vs. trough) alpha phase at stimulus onset. Results shown were per-voxel thresholded at $p < 0.005$ then cluster-thresholded at $p < 0.05$ and are displayed in radiological orientation on an MNI template brain. z coordinates are specified.

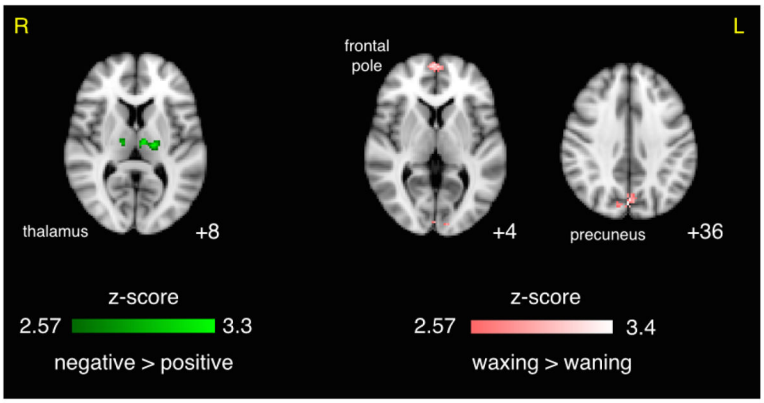

Figure 7. Effect of Prestimulus Alpha Phase on Decision-Related BOLD Activity

Results of paired t-test comparing the target vs. standard contrast for negative vs. positive (trough vs. peak) and waxing vs. waning alpha phase at stimulus onset. Results shown were per-voxel thresholded at $p < 0.005$ then cluster-thresholded at $p < 0.05$ and are displayed in radiological orientation on an MNI template brain. z coordinates are specified.

Table 1

Effect of Prestimulus EEG Alpha Power on BOLD Response to Auditory Targets and Task-Related Processing.

POWER

BOLD Response to Target Stimuli

contrast	Nvox	max z	$p_{cluster}$	MNIx	MNIy	MNIz	hem	region
high > low	25	3.02	0.0414	−38	−60	−42	L	cerebellum
low > high	190	3.69	0.0006	−6	−82	50	L	superior LOC, precuneus cortex
low > high	71	3.44	0.0049	−2	−62	60	L	precuneus cortex, superior LOC
low > high	63	3.20	0.0069	−32	−88	26	L	superior LOC, occipital pole
low > high	54	3.00	0.0099	−48	−70	−22	L	inferior LOC, inferior temporal gyrus
low > high	51	3.45	0.0098	−2	−86	−20	L/R	lingual gyrus, occipital fusiform gyrus
low > high	48	3.40	0.0105	28	−88	−4	R	LOC, occipital fusiform gyrus, occipital pole
low > high	35	3.13	0.0214	−2	−78	−4	L	lingual gyrus, intracalcarine cortex, occipital fusiform gyrus
low > high	33	2.98	0.0267	−20	−94	0	L	occipital pole, LOC
low > high	29	3.07	0.0333	−4	−44	8	L/R	PCC
low > high	26	3.27	0.0347	14	−42	−4	R	PCC, lingual gyrus, parahippocampal gyrus

Task Related BOLD Activity (Targets vs. Standards)

paired t-test	Nvox	max z	$p_{cluster}$	MNIx	MNIy	MNIz	hem	region
high > low	253	3.78	0.0003	−6	−4	46	L/R	cingulate gyrus
high > low	104	3.22	0.0028	−34	−22	46	L	postcentral gyrus, precentral gyrus
high > low	87	3.42	0.0036	48	40	4	R	frontal pole, inferior frontal gyrus
high > low	85	3.12	0.0040	−32	−18	70	L	precentral gyrus, postcentral gyrus
high > low	56	3.28	0.0094	−34	−36	48	L	postcentral gyrus
high > low	50	2.98	0.0113	50	10	30	R	precentral gyrus
high > low	42	2.87	0.0160	28	−38	54	R	postcentral gyrus
high > low	32	3.22	0.0236	−16	−84	26	L	superior LOC
high > low	30	3.10	0.0278	42	6	38	R	MFG, precentral gyrus, IFG
high > low	30	2.96	0.0298	16	−14	62	R	precentral gyrus
high > low	29	3.33	0.0298	30	−6	64	R	precentral gyrus, SFG, MFG
high > low	27	3.24	0.0343	−2	−14	60	L/R	precentral gyrus
high > low	26	3.11	0.0377	24	−16	72	R	precentral gyrus, SFG, postcentral gyrus

Task Related BOLD Activity (Targets vs. Standards)

paired t-test	Nvox	max z	$p_{cluster}$	MNIx	MNIy	MNIz	hem	region
high > low	25	2.98	0.0410	56	−6	−24	R	middle temporal gyrus
high > low	22	3.19	0.0470	−52	10	34	L	MFG, precentral gyrus, IFG

Per-voxel thresholded at $p < 0.005$ then cluster-corrected at $p < 0.05$. IFG = inferior frontal gyrus; LOC = lateral occipital cortex; MFG = middle frontal gyrus; PCC = posterior cingulate cortex; SFG = superior frontal gyrus.

Table 2

Effect of Prestimulus EEG Alpha Phase on BOLD Response to Auditory Targets and Task-Related Processing.

PHASE

BOLD Response to Target Stimuli

contrast	Nvox	max z	$p_{cluster}$	MNIx	MNIy	MNIz	hem	region
positive > negative	112	3.19	0.0027	6	−56	56	R	precuneus
positive > negative	80	3.10	0.0063	−38	−78	−26	L	cerebellum, occipital fusiform gyrus
negative > positive	109	3.55	0.0026	−18	−18	8	L	thalamus
negative > positive	43	3.25	0.0194	14	−16	6	R	thalamus
decreasing > increasing	39	3.20	0.0241	−38	−4	60	L	MFG, precentral gyrus

Task Related BOLD Activity (Targets vs. Standards)

paired t-test	Nvox	max z	$p_{cluster}$	MNIx	MNIy	MNIz	hem	region
negative > positive	118	3.30	0.0027	−18	−18	8	L	thalamus
negative > positive	61	2.98	0.0109	14	−16	8	R	thalamus
increasing > decreasing	26	3.30	0.0456	20	−14	−18	R	hippocampus, amygdala, parahippocampal gyrus
decreasing > increasing	34	2.94	0.0293	−40	−2	58	L	MFG, precentral gyrus, SFG
waxing > waning	240	3.40	0.0008	0	−74	36	L/R	precuneus cortex, cuneal cortex, superior LOC
waxing > waning	96	3.25	0.0038	4	60	4	L/R	frontal pole, paracingulate gyrus
waxing > waning	72	3.20	0.0082	−10	−94	6	L	occipital pole, supracalcarine cortex
waxing > waning	38	2.84	0.0270	4	−74	20	L/R	cuneal cortex, supracalcarine cortex

Per-voxel thresholded at $p < 0.005$ then cluster-corrected at $p < 0.05$. LOC = lateral occipital cortex; MFG = middle frontal gyrus; SFG = superior frontal gyrus.